invited

Modeling of Electronic States and Electron-Phonon Interaction in Quantum Dots

N. Mori, T. Ezaki†, and C. Hamaguchi

Department of Electronic Engineering, Osaka University,
2–1 Yamada-oka, Suita City, Osaka 565–0871, Japan
Phone: +81-6-879-7767, Fax: +81-6-879-7753
E-mail: mori@ele.eng.osaka-u.ac.jp

Electronic states in quantum dots containing N electrons are calculated by numerically diagonalizing the N-electron Hamiltonian in order to study the effect of the dot-shape on the electronic states. Energy relaxation time through longitudinal-acoustic phonon emission is also calculated using the exact eigen-states.

1. Introduction

Recent progress in micro-fabrication technology has enabled us to experimentally investigate quantum mechanics in semiconductor micro-structures such as quantum well, quantum wire and quantum dot (QD) in which the electron motion is restricted in two, one and zero dimension, respectively. Tarucha *et al.* [1] have reported experimental results on the tunnelling of electrons through a QD, and showed that the addition energy of an electron in the QD with several electrons is strongly affected by the electron-electron interaction. In QDs, it is pointed out that relaxation of electrons through the electron-phonon interaction is reduced because of the discrete energy levels [2, 3]. For a QD with more than one electron, however, the Coulomb interaction between electrons results in complicated and dense electronic structures, which may affect the relaxation process. In the present study, we have performed an exact diagonalization for the N-electron states in a QD, and calculated the relaxation time from the excited states to the ground state via longitudinal-acoustic (LA) phonon emission.

2. Model and Method

A schematic illustration of the model for a QD formed in a vertical $In_xGa_{1-x}As$/AlGaAs heterostructure [1, 4] is shown in Fig. 1. The x–y plane and the z direction are taken to be parallel and perpendicular to the heterointerfaces, respectively. In the model, electrons are assumed to be confined by the potential well, $H(z)$, due to the heterojunctions along the z direction. We model the lateral confining potential $V(x,y)$ by the following equation

$$V(x,y) = \frac{1}{2}m^*(\omega_x^2 x^2 + \omega_y^2 y^2)\left\{1 + \alpha\frac{2}{7}\cos 3\phi\right\}, \quad (1)$$

where ω_x and ω_y are the confining energies along the x and y directions, respectively, α (= 0 or 1) is a parameter to specify the shape of the lateral confining potential, and ϕ is the angle with respect to the specific axis in the x–y plane. When $\alpha = 0$, the contour line of the lateral confining potential becomes an ellipse (for $\omega_x \neq \omega_y$) or a circle (for $\omega_x = \omega_y$). A triangular shaped confining potential can be obtained by setting 1 for the parameter α and putting $\omega_x = \omega_y$.

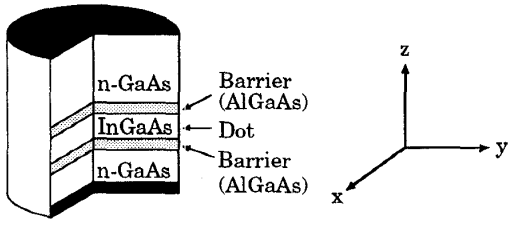

Figure 1 Schematic diagram of a vertical quantum dot structure together with the coordinate system used in the present study. The x–y plane and the z direction are taken to be parallel and perpendicular to the heterointerface, respectively.

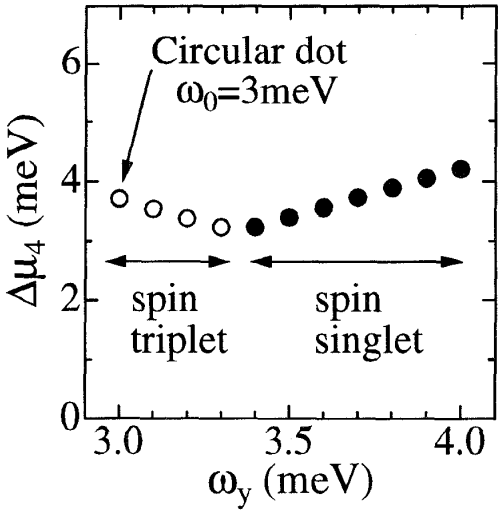

Figure 2 Addition energy $\Delta\mu_4$ as a function of the confining energy of ω_y keeping the average confining energy a constant value of $(\omega_x + \omega_y)/2 = 3\,\mathrm{meV}$.

0-7803-4369-7/98 $10.00

The N-electron Hamiltonian can then be written as follows

$$\mathcal{H} = \sum_{i=1}^{N} \mathcal{H}_0(\boldsymbol{r}_i) + \sum_{i<j} \frac{e^2}{4\pi\epsilon|\boldsymbol{r}_i - \boldsymbol{r}_j|}, \qquad (2)$$

where $\mathcal{H}_0(\boldsymbol{r}) = \boldsymbol{p}^2/2m^* + V(x,y) + H(z)$ is the single-electron Hamiltonian. We expand the N-electron states by the Slater determinants, which are constructed by an appropriate single-particle eigen-functions, and calculate the N-electron states by numerically diagonalizing the Hamiltonian of Eq. (2) [5]. The relaxation time through LA phonon emission is then calculated by using the Fermi's golden rule with the exact N-electron states [6].

3. Electronic States

Figure 2 shows the addition energy $\Delta\mu_4$ as a function of the confining potential of ω_y keeping the average confining energy a constant value of $(\omega_x + \omega_y)/2 = 3\,\mathrm{meV}$. $H(z)$ is assumed to be an infinite square potential well of width $a = 12\,\mathrm{nm}$ for simplicity. Open and solid circles correspond to the spin triplet and the spin singlet ground state for the QD containing four electrons, respectively. For elliptic shaped QDs with weak asymmetry ($3\,\mathrm{meV} < \omega_y \lesssim 3.3\,\mathrm{meV}$), the spin triplet states remain the lowest eigen-state, and the addition energy decreases with increasing the asymmetry due to the removal of the degeneracy of the single-particle states. For QDs with $\omega_y > 3.3\,\mathrm{meV}$, the spin singlet state becomes the ground state, and the addition energy increases with increasing ω_y. This may be explained by considering the following fact. With increasing the asymmetry of the confining potential in the x–y plane, a disk-like QD approaches to a needle-like QD as shown in Fig. 3 where we plot the density of electrons in QDs containing three electrons for the circular and the elliptic shaped QDs, and the complete shell filling may take place in a needle-like QD with four electrons.

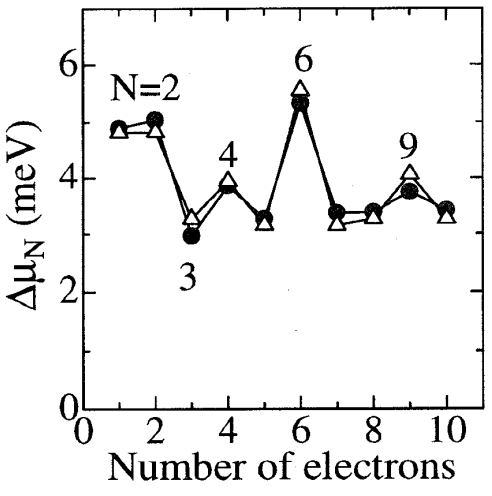

Figure 4 Addition energy in a circular shaped quantum dot (●) and a triangular shaped quantum dot (△) as a function of the number of electrons. $\omega_0 = 3\,\mathrm{meV}$.

Figure 4 shows the N dependence of addition energy for a triangular shaped QD with $\omega_0 \equiv \omega_x = \omega_y = 3\,\mathrm{meV}$, where the result of the circular shaped QD are plotted by solid circles for comparison. In Fig. 4, the addition energies of the circular and the triangular shaped QDs are found to exhibit almost

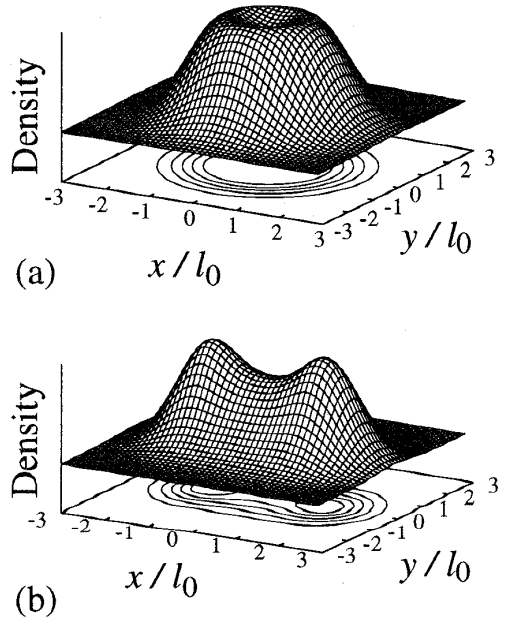

Figure 3 Density distribution of electrons in a quantum dot containing three electrons with a circular ($\omega_x = \omega_y = 3\,\mathrm{meV}$) (a), and an elliptic ($\omega_x = 2\,\mathrm{meV}$, $\omega_y = 4\,\mathrm{meV}$) (b) shaped confining potential. ℓ_0 is 20 nm.

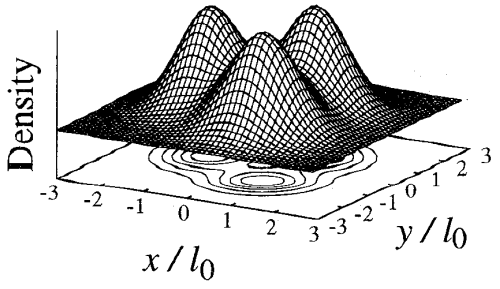

Figure 5 Density distribution of electrons in a quantum dot containing three electrons with a triangular shaped confining potential. ℓ_0 is 20 nm.

the same characteristics. The addition energy $\Delta\mu_N$ of the triangular shaped QD for $N = 3$, 6 and 9, however, is found to be slightly larger than that of a circular shaped QD. These features may be explained as follows. The density of electrons in QDs containing three electrons is shown in Fig. 3(a) for the circular shaped QD and Fig. 5 for the triangular shaped QD. As seen in Fig. 3(a), electrons in the circular shaped lateral potential form a rotationally symmetric distribution, and the electron density becomes small in the center of the QD due to the electron-electron repulsion. On the other hand, in the triangular shaped QD, each electron moves toward each corner of the triangle and forms more stable state as shown in Fig. 5, giving rise to a slightly larger addition energy. For the same reason electronic states for $N = 6$ and 9 in the triangular shaped QD form slightly stable states compared to the case of the circular shaped QD.

4. Relaxation Time

4.1. Triangular-Well Quantum Dots

Electron relaxation time, τ, via LA phonon emission from the excited states to the ground state is calculated by using the exact electronic states within the frame of the Fermi's golden rule. Figure 6 shows the relaxation time, τ, as a function of the energy difference, $\varepsilon_i - \varepsilon_0$, between the excited states and the ground state for a quantum dot with a triangular well in the z direction and a circular shaped confinement in the x–y plane. The triangular shaped confining potential of $H(z)$ is taken into account by setting the single-particle wave function associated with the quantized z-motion to the Fang-Howard trial function

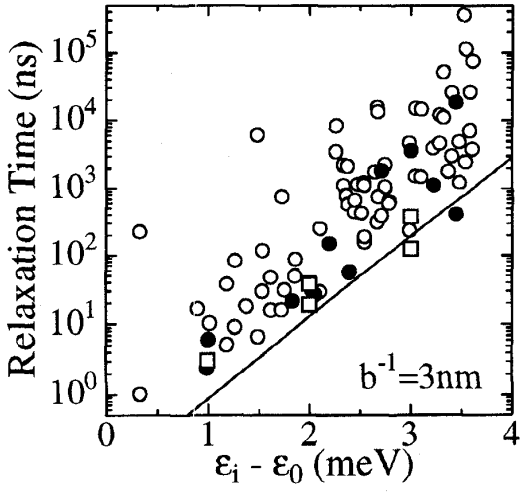

Figure 6 Relaxation time as a function of the energy difference between the initial states and the final ground state for a quantum dot with $b^{-1} = 3\,\text{nm}$ containing one electron (□), two electrons (●), and three electrons (○). The solid line corresponds to the approximate relaxation time given by Eq. (3).

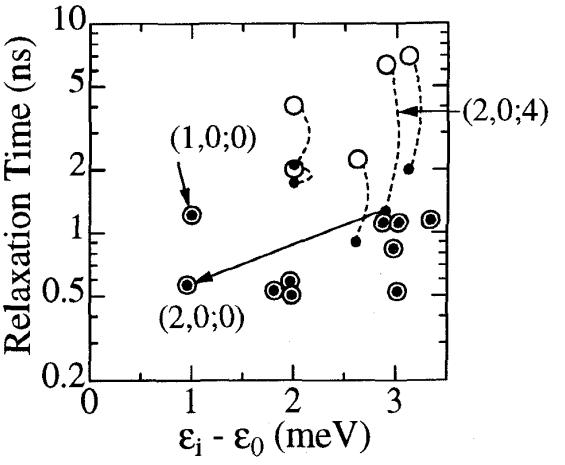

Figure 7 Relaxation time as a function of the energy difference between the initial states and the ground state for a two-electron quantum dot with $a = 5\,\text{nm}$. Large open circles and small solid circles correspond to the direct and the fastest relaxation processes, respectively.

of $\propto z\exp(-\frac{1}{2}bz)$ [7]. Because of the strong confinement along the z direction of $b^{-1} = 3\,\text{nm}$ in Fig. 6, τ increases exponentially with $\varepsilon_i - \varepsilon_0$. The electron-electron interaction makes the electronic states dense and complicated, but the relaxation time is found to mainly depend on the energy difference of $\Delta\varepsilon \equiv \varepsilon_i - \varepsilon_0$, and its dependence is approximately expressed as

$$\tau(\Delta\varepsilon) = \frac{4\sqrt{2}\pi\hbar d c_s^2}{\ell_0 D^2 b^4} \exp\left\{\left(\frac{2.8}{b} + 3\ell_0\right)\frac{\Delta\varepsilon}{\hbar c_s}\right\} \quad (3)$$

with $\ell_0 = (m\omega_0/\hbar)^{1/2}$, D being the deformation potential, d the density of the material, and c_s the speed of sound. Since

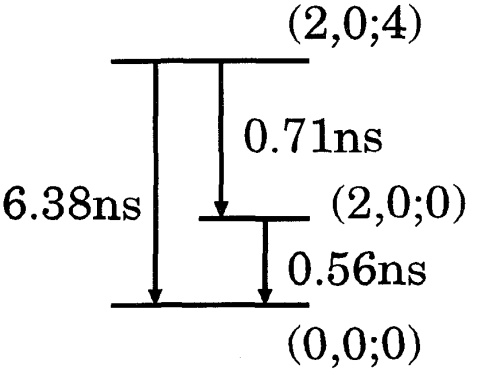

Figure 8 A schematic diagram for the direct and the fastest relaxations from the initial state $(2, 0; 4)$.

the electronic states become dense for many electrons' systems, the relaxation time may become faster with increasing the number of electrons.

4.2. Square-Well Quantum Dots

Figure 7 shows the relaxation time, τ, as a function of the energy difference between the excited states and the ground state in a two-electron QD with a circular shaped confinement, $V(x,y)$, of $\omega_0 = 1\,\mathrm{meV}$ and a square well, $H(z)$, of $a = 5\,\mathrm{nm}$, where open and solid circles correspond to the direct and the fastest processes, respectively. The direct process is an one-phonon process, while the fastest process may involve many phonons. The indices $(\mathcal{M}, \mathcal{S}_z; \mathcal{N})$ are quantum numbers of eigen-states, indicating the $\mathcal{N}$-th state of the N-electron states with a total angular momentum $\hbar\mathcal{M}$ and a total spin along the z direction $\hbar\mathcal{S}_z/2$. The connected pairs of an open circle and a solid circle indicate the relaxation from the same initial states, and imply the existence of faster indirect process, *i.e.* the electron pass through certain intermediate state(s) before relaxing to the grand state, whereas the open circles with a solid circle indicate that the fastest process is the direct process.

A typical relaxation process from $(2,0;4)$ state is illustrated in Fig. 8. The fastest indirect transition arises from the scattering process via the state $(2,0;0)$. The relaxation time for the direct process is about 6.38 ns, whereas the relaxation time for the indirect process is 1.27 ns which is given by the sum of 0.71 ns for the scattering from $(2,0;4)$ to $(2,0;0)$ and 0.56 ns for the scattering from $(2,0;0)$ to the ground state $(0,0;0)$. From a study of the N and a dependences of the relaxation time, we find that there are two types of the fastest indirect processes. One is the process where the transition occurs between the initial and the final N-electron states ($N \geq 2$) in which two or more single particle states in the main contribution to the N-electron states differ from each other. The other is the process between the states with the energy separation greater than the maximum phonon energy $\varepsilon_{\max}$, which will be defined and explained later. In a QD with $a = 5\,\mathrm{nm}$ shown in Fig 7, $\varepsilon_{\max} = 4.3\,\mathrm{meV}$ and the fastest indirect processes arise from in the former mechanism.

The maximum phonon wave vector is given by $q_{\max} = 2\pi/a$, which gives the maximum phonon energy $\varepsilon_{\max} = \hbar c_s q_{\max}$ [8]. The maximum phonon energies are $\varepsilon_{\max} = 4.3$, 2.2 and 1.1 meV, which are indicated by arrows on the horizontal axises in Fig. 9, for $a = 5$, 10 and 20 nm, respectively. Relaxation processes from the excited states with $\varepsilon_i - \varepsilon_0 > \varepsilon_{\max}$ are strongly suppressed in a QD with single electron. As can be seen in Fig. 9, this suppression is found to occur in a QD with a few electrons. We also find that several relaxation processes are accelerated through the certain intermediate state(s) between the initial and the final ground states even for $\varepsilon_i - \varepsilon_0 < \varepsilon_{\max}$.

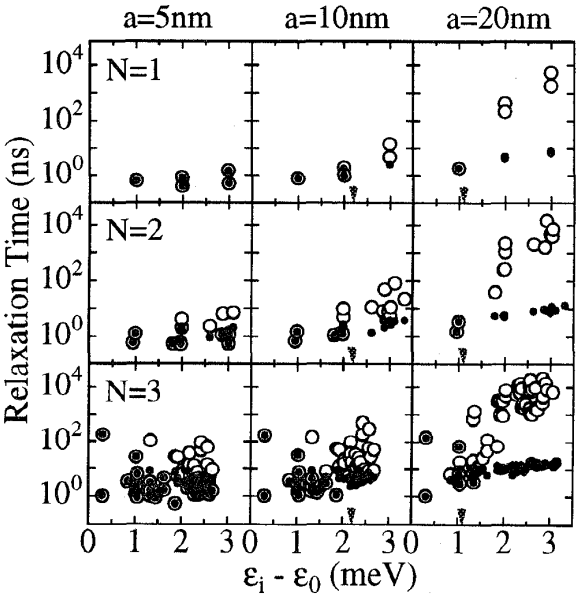

Figure 9 Relaxation time from excited states to the ground state through longitudinal-acoustic phonon emission as a function of the energy difference for circular shaped quantum dots with $\omega_x = \omega_y = 1\,\mathrm{meV}$ and $a = 5$, 10 and 20 nm. Open and solid circles correspond to the direct (one-phonon) process and the fastest process, respectively.

5. Summary

The N-electron eigen-states were calculated by the exact diagonalization method in QDs with lateral confinement of circular, elliptic and triangular shaped potentials, and studied the effect of the dot-shape on the electronic states. Electron relaxation time toward the ground state via LA-phonon emission in QDs containing N electrons was also calculated. We find that several relaxation processes are accelerated through the certain intermediate state(s) between the initial and the final states.

References

† Present address: ULSI Research Laboratory, Silicon Systems Research Laboratories, NEC Corporation, 1120, Shimokuzawa, Sagamihara, Kanagawa 229-1198, Japan.

[1] S. Tarucha, D.G. Austing, T. Honda, R.J. van der Hage, and L.P. Kouwenhoven, Phys. Rev. Lett. **77**, 3613 (1996).

[2] U. Bockelmann and G. Bastard, Phys. Rev. B, **42**, 8947 (1990).

[3] H. Benisty, C.M. Sotomayor-Torrès, and C. Weisbuch, Phys. Rev. B, **44**, 10945 (1991).

[4] D.G. Austing, T. Honda, and S. Tarucha, Semcond. Sci. Technol. **11**, 388 (1996).

[5] T. Ezaki, Y. Sugimoto, N. Mori, and C. Hamaguchi, Physica B **249–251**, 238 (1998).

[6] T. Ezaki, N. Mori, and C. Hamaguchi, Phys. Stat. Sol. (b) **204**, 272 (1997).

[7] F.F. Fang and W.E. Howard, Phys. Rev. Lett., **16**, 797 (1966).

[8] H. Benisty, Phys. Rev. B, **51**, 13281 (1995).